Biomed Microdevices
DOI 10.1007/s10544-014-9874-0

Electrical cell counting process characterization in a microfluidic impedance cytometer

Umer Hassan · Rashid Bashir

Abstract Particle counting in microfluidic devices with coulter principle finds many applications in health and medicine. Cell enumeration using microfluidic particle counters is fast and requires small volumes of sample, and is being used for disease diagnostics in humans and animals. A complete characterization of the cell counting process is critical for accurate cell counting especially in complex systems with samples of heterogeneous population interacting with different reagents in a microfluidic device. In this paper, we have characterized the electrical cell counting process using a microfluidic impedance cytometer. Erythrocytes were lysed on-chip from whole blood and the lysing was quenched to preserve leukocytes which subsequently pass through a 15 μm×15 μm measurement channel used to electrically count the cells. We show that cell counting over time is a non-homogeneous Poisson process and that the electrical cell counts over time show the log-normal distribution, whose skewness can be attributed to diffusion of cells in the buffer that is used to meter the blood. We further found that the heterogeneous cell population (i.e. different cell types) shows different diffusion characteristics based on the cell size. Lymphocytes spatially diffuse more as compared to granulocytes and monocytes. The time difference between the cell occurrences follows an exponential distribution and when plotted over time verifies the cell diffusion characteristics. We also characterized the probability of occurrence of more than one cell at the counter within specified time intervals using Poisson counting statistics. For high cell concentration samples, we also derived the required sample dilution based on our particle counting characterization. Buffer characterization by considering the size based particle diffusion and estimating the required dilution are critical parameters for accurate counting results.

Keywords Microfluidic impedance cytometer · Poisson statistics · Blood cell counting · Buffer characterization

1 Introduction

Particle counting using coulter principle has been around since 1953 (Coulter 1953) and finds many biological and industrial applications. For biological applications, coulter counting has been used to detect particles such as pollen (Zhang 2005), bacteria (DeBlois 1977), DNA (Kasianiwicz 1996) using nano-pores and antigen- antibody (Saleh 2003) can also be detected using on-chip nano-pores. The recent advances in the MEMS technology and rapid prototyping, results in making the microfluidic particle counters based on coulter detection principle (Sun 2010). Such sensors are being used for a range of applications including purification of liquids by determining the size distribution of the particles inside the sample, enumerating yeast cells in the brewing industry (Teass 1998) and for counting somatic cells in milk (Phipps and Newbould 1996). Other examples include, particle size determination in composition analysis of debris while using atomic emission

Electronic supplementary material The online version of this article (doi:10.1007/s10544-014-9874-0) contains supplementary material, which is available to authorized users.

U. Hassan · R. Bashir
Department of Electrical and Computer Engineering, William L. Everitt Laboratory, University of Illinois at Urbana-Champaign, 1406W Green St., Urbana, IL 61801, USA

U. Hassan · R. Bashir
Micro and Nanotechnology Lab, University of Illinois at Urbana-Champaign, 208 N. Wright St., Urbana, IL 61801, USA

R. Bashir (✉)
Department of Bioengineering, 1270 Digital Computer Laboratory, University of Illinois at Urbana-Champaign, 1304W. Springfield Ave., Urbana, IL 61801, USA
e-mail: rbashir@illinois.edu

Published online: 05 June 2014

spectroscopy (Kauffman 1989) and event detection systems with Geiger tubes (Arqueros 2004; Leo 1994).

Cell counting in microfluidic chips can be done by passing a cell through a coulter aperture with co-planar or top-bottom electrodes bonded to it (Holmes 2009). Many studies have been done to count different cell types including leukocytes, monocytes, platelets, erythrocytes (Berkel et al. 2011; Cheung 2010; Holmes 2010). Cell counting in a coulter counter follows the Poisson statistics. However, its detailed characterization is critical in accurate cell counting in microfluidic devices. In high cell concentration samples e.g. in erythrocyte counting from diluted whole blood (Berkel 2011), a portion of the sample is considered for cell counting because of high volume of total sample after dilution. In such applications, the cell counts assume to follow uniform distribution throughout the experiment. However, as we will show in this article, the distribution depends on the effectiveness of the buffer pushing the sample, or else the cells gets diffused into the buffer and cell counts doesn't follow the uniform distribution over time. This makes the sample portion selection very critical. Another important parameter to characterize is to find the amount of the dilution required for accurate cell counting as this limits the time, throughput, power and the amount of the reagents used in the device.

Recently, we have developed a microfluidic impedance cytometer for HIV/AIDS diagnostics (Hassan 2014; Watkins 2013, 2011). It takes a small volume of whole blood (10 μL) and count the CD4+ and CD8+ T cells with high accuracy at point-of-care. Using that biochip, here we have given a complete characterization of the cell counting process. Our electrical cell counter is based on co-planar electrodes bonded with 15 × 15 μm cross-sectional area of the microfluidic measurement channel. In this biochip, erythrocytes were lysed from whole blood and remaining leukocytes comprising of mainly lymphocytes, granulocytes and monocytes were electrically counted. We have characterized the cell counting process over time as a non-homogenous Poisson process and shown that this charcaterization is useful for buffer characterization, required sample dilution estimation and accurate cell counting.

2 Experimental setup

2.1 Protocol

The schematic of the microfluidic impedance cytometer is shown in Fig. 1a. The 10 μL of whole blood is infused at one of the three inlet ports (represented by red color). The lysing reagent composed of 0.12 % (v/v) formic acid and 0.05 % (w/v) saponin in DI water is infused at yellow port. The mixing of the blood with the lysing buffer in the lysing region resulted in complete lysis of erythrocytes. The quenching buffer composed of 5.3 mL of 0.6 % (w/v) sodium carbonate and 3 % (w/v) sodium chloride in DI water is infused at blue inlet port to stop the lysing process and maintain the osmolarity and pH of the solution (Hassan 2014; Watkins 2013). The quenched sample flow through the 15 × 15 μm^2 cross-sectional cell counting channel with microfabricated electrodes aligned with it. Fig. 1a also shows the typical leukocytes passing through the cell counting channel represented by blue circles. As each cell pass through the microfabricated electrodes, it generates a bipolar voltage pulse, with pulse amplitude proportional to the cell size and pulse width to the cell's velocity. Fig. 1b shows the typical voltage signal acquired during the cell counting experiment for 2 sec. Many cells pass through the counting channel as seen by the many bipolar pulses. Fig. 1c shows a typical bipolar voltage pulse generated at each cell passage. All the bipolar voltage pulses are recorded above 3 times standard deviation of noise and a pulse amplitude histogram is plotted as shown in Fig. 1d. The dotted rectangular region shows the two leukocyte sub-populations which includes lymphocytes and granulocytes + monocytes. The left population in the dotted rectangle represents the lymphocyte population as they are smaller in size with almost 7.8 μm average diameter (Hassan 2014) as compared to granulocytes + monocytes with almost 12 μm average cell diameter. The left region to the dotted rectangle is erythrocyte debris. The rectangular leukocyte region is selected by considering the minima in between the debris and lymphocyte population.

2.2 Chip fabrication

Twenty five nanometers Ti (adhesion layer) and 75 nm Pt (conduction layer) is evaporated and patterned on the Pyrex glass substrate. The undesired metal is lifted off using standard metal lift-off technique to make the final Platinum electrodes. SU-8 50 negative photoresist is patterned on a Si wafer to make negative master, to which polydimethylsiloxane (PDMS) was poured and then cured to make the microfluidic channels (Hassan 2014; Watkins 2013). The cured PDMS chips were permanently bonded with glass electrodes using oxygen plasma.

2.3 Blood samples acquisition

We collected blood samples for this study from University of Illinois student volunteers through an Institutional Review Board (IRB) approval. Blood was drawn by a trailed phlebotomist via venipuncture and collected in EDTA-coated BD Vacutainers (BD Biosciences). Afterwards, the sample is kept on rotisserie at room temperature. Experiments were performed within a few hours of the blood draw.

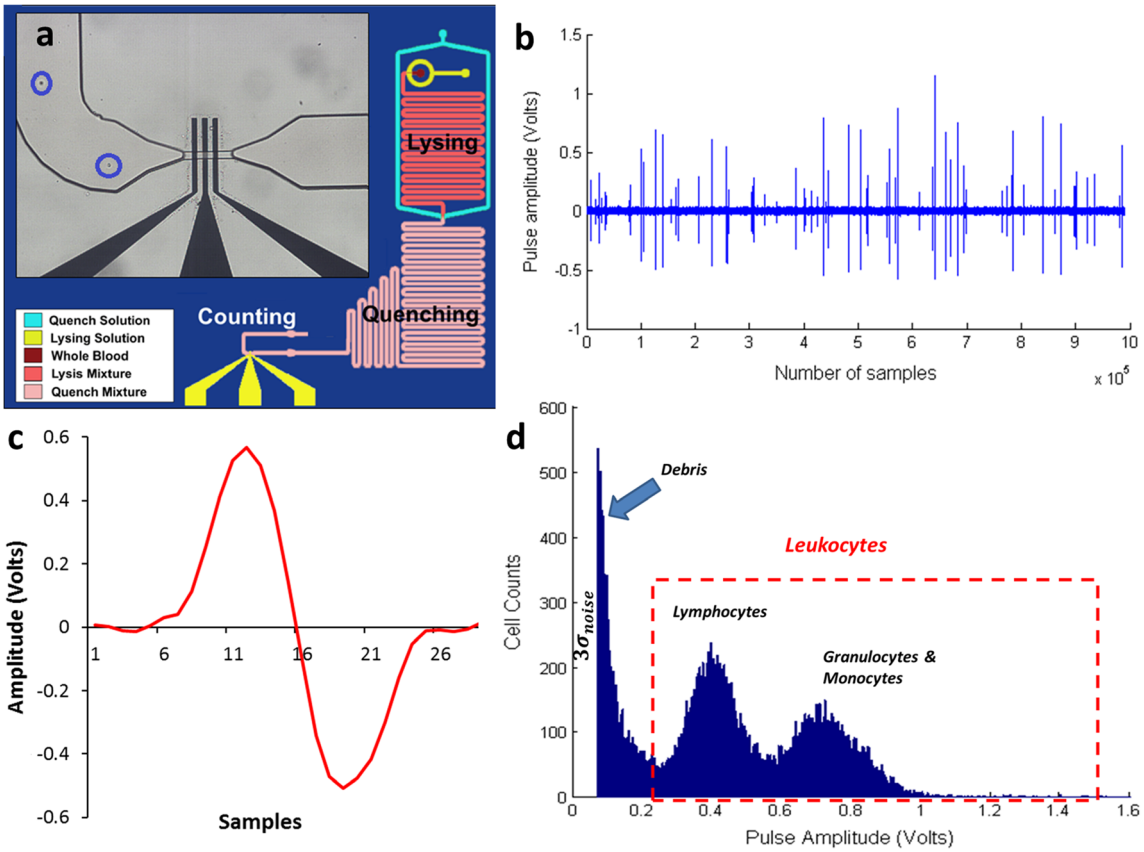

Fig. 1 Experimental Setup (Hassan 2014). **a** The device layout with lysing and quenching modules is shown. Blood, lysing and quenching solutions are represented by different colors at their respective infusion ports. The "Lysing" indicates the region where blood and lysing buffer mixed to lyse all erythrocytes. The "Quenching" indicates the region where quenching buffer gets mixed to maintain the osmolarity of the solution. The zoomed-in version of yellow electrodes shows the cell counting region of 15×15 um^2 cross-section with electrodes aligned with it. The blue circles show the typical leukocytes passing through the measurement channel. **b** The bipolar pulses for each passage of a cell, with height of the pulse proportional to the cell size and width to the cell's velocity. **c** A typical bipolar voltage pulse. **d** All the voltage bipolar pulses are recorded above 3 times standard deviation of noise and a pulse amplitude histogram is plotted. The dotted rectangular region shows the two leukocyte populations including lymphocytes and granulocytes+ monocytes. The left region to the dotted rectangle is erythrocyte debris and the rectangular leukocyte region is selected by considering the minima in between the debris and lymphocyte population

3 Results

3.1 Cell diffusion characterziation

Ten microliters of whole blood is infused with lysing and quenching buffers with ratios of blood: lysing (1:12) and blood: quenching (1:6.3) (Watkins 2013). The ratios were optimized for the maximum recovery of leukocytes after erythrocyte lysis. The electrical counts were obtained for the entire experiment duration of 15 min. The entire duration is divided into 100 time intervals and histogram is plotted for the cell counts w.r.t experiment time and is shown in Fig. 2a. Cell count distribution over time shows the log-normal function with characteristic value of μ=1.644 and σ=0.3728. It is given by the following Eq. 1.

$$y = f(t \mid \mu, \sigma) = \frac{1}{t\sigma\sqrt{2\pi}} e^{\frac{-(\ln t-\mu)^2}{2\sigma^2}} \quad (1)$$

The log-normal cell counting distribution can be explained by the cell diffusion in the buffer as shown in the conceptual illustration in Fig. 2b. The cell counts over the experiment duration were expected to follow a uniform distribution. However, we see a very rapid increase in the cell counts during the start of the experiment and a slow decrease in the cell counts at the end of the experiment. The 'buffer' in Fig. 2b represents both lysing and quenching solutions together. Before the blood starts to flow in the bio-chip, a buffer is already flowing in the bio-chip. The buffer solution interacts with the blood allowing the cells to diffuse and allowing some cells to appear early. The mass transfer coefficient given by $k=D/\delta$ depends on diffusion coefficient, D and depth of diffusion layer δ (Glaser 1993). The mass transfer coefficient at the start of the experiment k_s is lower than its value at the end of the experiment k_e, as the depth of the diffusion layer is greater at the start. This in turn results in higher rate of flow of cells to the buffer, v_m at the

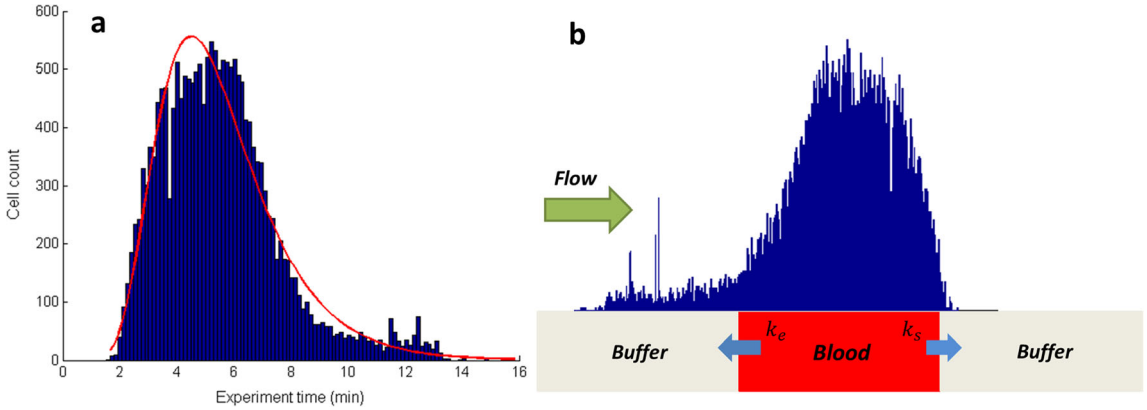

Fig. 2 **a** Histogram representing the electrical cell counts throughout the entire experiment time. The histogram shows the log-normal function (μ=1.644 and σ=0.3728). **b** Conceptual illustration of the log-normal cell distribution. The buffer interacts with the blood at start and end of blood infusion and results in diffusion of cells

end of the blood infusion. Mathematically this can be written as (Glaser 1993),

$$v_m = kA\left([Mol_{blood}] - [Mol_{buffer}]\right) \tag{2}$$

Where A is the cross-sectional area of the channel, $[Mol_{blood}]$ is the number of cells in blood and $[Mol_{buffer}]$ is the number of cells in the buffer after diffusion.

3.2 Diffusion characterization with heterogeneous cell population

The mean value of the log-normal distribution, μ, of cell counts decreases with the increase in the flow rate with an R^2 value of 0.96 as shown in Fig. 3a. This decrease can be associated with the decrease in the total experiment time as the flow rate is increased while using the same volume of blood sample i.e. 10 μL. Fig. 3b shows the histogram of the lymphocytes and granulocytes + monocytes cell counts over the experiment duration. The diffusion coefficient $D = \frac{kT}{6\pi\eta r}$ depends of the size of the particles/cells. Lymphocytes being smaller in size, have a higher diffusion coefficient of 41.40 fm^2/sec as compared to granulocytes + monocytes with value of 26.91 fm^2/sec. The higher diffusion coefficient, D for lymphocytes results in higher value of mass transfer coefficient k, which in turn increases the rate of flow of lymphocytes (v) to the buffer as compared to granulocytes + monocytes. This results in a more skewed distribution for the lymphocytes as compared to granulocytes + monocytes as shown in Fig. 3b. The μ value of the log-normal distribution decreases linearly with the increase in the flow rate for lymphocytes with an R^2 value of 0.92 and granulocytes + monocytes with an R^2 value of 0.98 as shown in Fig. 3c. This decrease can be associated with the decrease in the total experiment time as the flow rate is increased while using the same sample volume. The skewness of the log-normal function written in Eq. 1 is given as $\left(e^{\sigma^2}+2\right)\sqrt{(e^{\sigma^2}-1)}$, and gives a high value for lymphocytes as they get diffused more as compared to granulocytes + monocytes. Fig. 3d plots the skewness of the log-normal distribution for leukocytes, lymphocytes and granulocytes + monocytes. The skewness decreases linearly with increasing flow rates for leukocytes, lymphocytes and granulocytes + monocytes with an R^2 values of 0.94, 0.92, and 0.98 respectively. The high skewness for lymphocytes verifies that they get more diffused in the buffer as compared to granulocytes + monocytes as shown in Fig. 3d.

3.3 Cell counting characterization as a poisson process

Cell counting process can be mathematically related to a Poisson process (Kingman 1993). A Poisson process is a stochastic process which counts the number of events and the time of each event with respect to each other in a given time interval. Figure 4a shows a graphical depiction of a Poisson process which shows that the number of the cell counts (events) X, in the interval t_1 to t_2, follows the Poisson distribution with a parameter value λ, as given by the following equation.

$$y = P(X = k) = \frac{\lambda^k e^{-\lambda}}{k!} \tag{3}$$

A Poisson process can be subdivided into sub-Poisson processes for different time intervals as shown in Fig. 4b. If the values of λ are same for sub-processes, the entire process is a homogenous Poisson process, for different values of λ the process is called a non-homogeneous Poisson process (Ross 2006). The cell counting process of our experiment is a non-homogenous Poisson process, as the total number of cell counts changes over time throughout the experiment as we have shown in Fig. 2a. The cell counting process for the entire experiment is divided into sub-processes of 1 min time interval, which can be represented as Poisson processes as the cell counts follows the

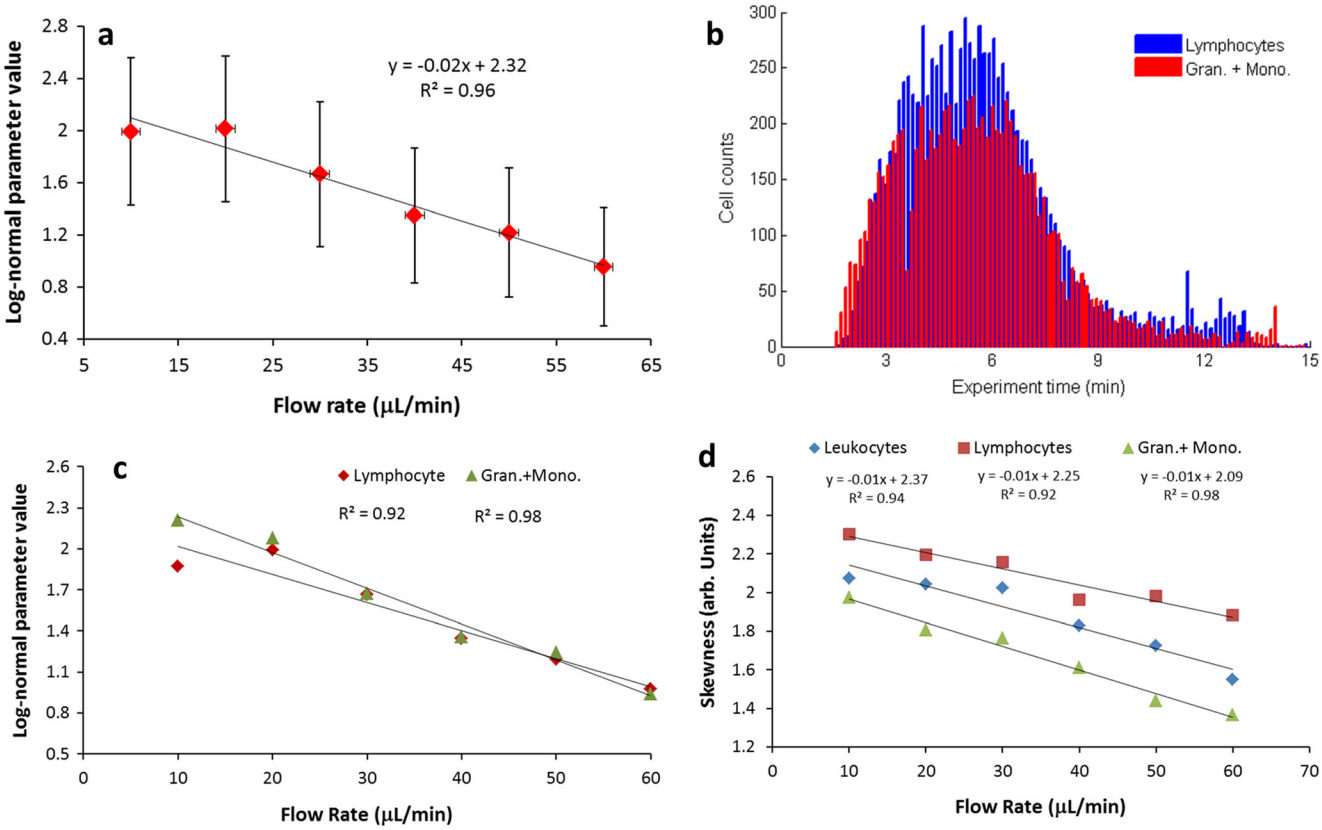

Fig. 3 **a** The μ value of the log-normal distribution of cell counts decreases with the increase in the flow rate as the experiment time is reduced (R^2=0.96). Error bars represents one standard deviation of the log-normal distribution at each flow rate. **b** Shows the histogram of the lymphocytes and granulocytes+monocytes cell counts over the experiment duration. The lymphocytes showed greater skewed distribution as compared to granulocytes+monocytes. **c** Shows the decrease in the μ value of the log-normal distribution of lymphocytes (R^2=0.92) and granulocytes+monocytes (R^2=0.98) with the increase in the flow rate as the experiment time is reduced. **d** The skewness of the log-normal distribution decreases with increasing flow rates for lymphocytes (R^2= 0.94) and granulocytes+monocytes (R^2=0.98). The lymphocytes show higher skewness as compared to granulocytes+monocytes as they get more diffused in the buffer

Poisson distribution in those sub processes. Fig. 4c shows the number of cell counts in time interval of 5 to 6 min which can be approximated as the uniform occurrence of cell counts for this entire duration. The 5–6 min duration is divided into 1000 intervals and number of cells were calculated in each interval. The corresponding Poisson distribution of the cell counts in interval 5–6 min is shown in the Fig. 4d with a λ value of 4.

3.4 Cell counting experiment, a non-homogeneous poisson process

The cell counting process for the experiment duration is represented as a non-homogeneous Poisson process by the following mathematical relation,

$$\int_{m=1}^{t_e} \frac{(\lambda_m t)^n e^{-\lambda t}}{n!}\, dm \tag{4}$$

Where t_e is the total experiment duration in minutes, and dm is the time interval for the sub- process which follows the Poisson distribution for the cell counts, in our case 1 min. The λ value is time dependent as the total number of cell counts differs at different times during an experiment as shown in Fig. 2a. The λ value is calculated for duration of 1 min throughout the experiment and is shown in Fig. 5. The λ value for lymphocytes is slightly greater than granulocytes + monocytes because of their slightly higher concentration in the sample after blood lysing. The λ value can be represented as a log-normal function whose μ value depends on the flow rate and the sample volume used for the experiment.

3.5 Inter-cell spacing characterization

The inter-event spacing of the Poisson process should follow the exponential distribution as shown in inset of Fig. 6a. The time difference in between the cell occurrences should follow the exponential distribution which can be given by the following equation,

$$y = f(t|\mu) = \frac{1}{\mu}\, e^{\frac{-t}{\mu}} \tag{5}$$

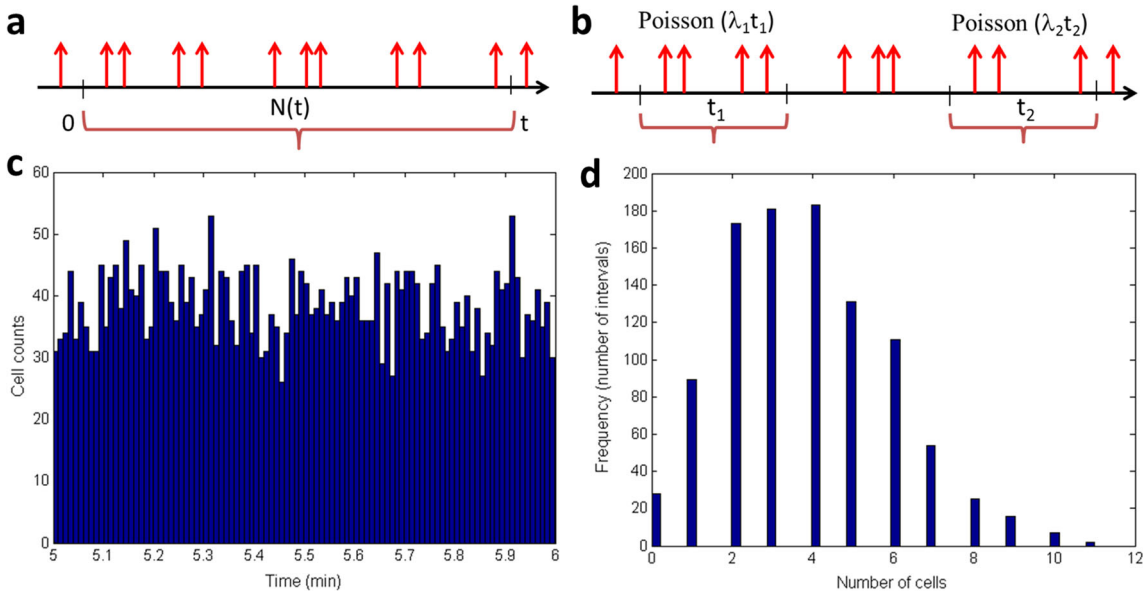

Fig. 4 **a** Poisson process describes the number of cell counts in a particular time interval. N (t) is the number of counts in the interval 0 to t, obeys the Poisson distribution. **b** A poisson process can be subdivided into sub-poisson processes for different time intervals e.g. t_1 or t_2. If the values of λ are same for sub-processes, the entire process is homogenous poisson process, for different values of λ the process is called non-homogeneous poisson process. The cell counting process is a non-homogenous poisson process. **c** The number of cell counts in time interval 5 to 6 sec (bins=200). **d** The Poisson distribution of the cell counts in interval 5–6 sec with a λ value of 4

The inter-cell spacing of total leukocytes (*N*=18599), lymphocytes (*N*=10188) and granulocytes + monocytes (*N*=8411) follows exponential distribution with μ values as 47.42, 86.43 and 79.02 ms respectively as shown in Fig. 6a. The μ value increases as the number of the cells decreases in the solution. As the experiment progresses in time, the μ value of exponential distribution for an increment of 1 min would decrease. Figure 6b shows this decrease in the inter-cell time spacing for leukocytes, lymphocytes and granulocytes + monocytes. No cells appear for initial 2 min after the blood infuses into the chip and lysing and quenching process initiates as represented by (A) in Fig. 6b. Cells gets diffused in buffer resulting in higher inter-cell time spacing of almost 1 sec as the cells starts to appear at the counting region (B) comprising only of lymphocytes. Granulocytes + monocytes appeared 30 sec late (C), as they get diffused less as compared to lymphocytes. Granulocytes + monocytes stops appearing 3 min before the end of the experiment (D) as compared to lymphocytes as a result of less diffusion into the buffer.

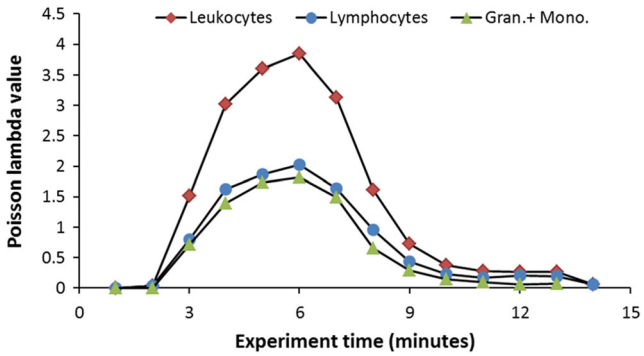

Fig. 5 The cell counting process for the experiment duration is a non-homogeneous poisson process. The plot represents the λ value for duration of 1 min throughout the experiment. The λ value for lymphocytes is slightly greater than granulocytes+monocytes because of their slightly higher concentration in the sample after blood lysing

3.6 Doublet/Triplet characterization (Poisson bursts/clumping)

It is the characteristic of the Poisson process that the random events occurs in bursts or clumps i.e. more than one event occur in a specified interval. The probability of getting Poisson clumps can be obtained from Eq. 3, where λ is the average number of events occurring in the specified time interval and *k* is the number of "event clumps" occurred in that time interval. Figure 7a shows the conceptual schematic for the occurrence of event clumps in specified time intervals, which follows a Poisson probability function. Entire experiment duration is divided into the time intervals of 120 s. Figure 7b shows the Poisson distribution of cell counts for interval of 120 sec during 5–7 min of experiment duration. The time interval for which average number of events is 1 i.e. λ=1, is found by dividing the total time of 120 s with the total number of cells occurring in this duration. Using Eq. 3, the probability of 0, 2 (doublet) and 3 (triplet) cells appearing for the entire experiment duration of 15 min is shown in Fig. 7c. The solid black lines represent the theoretical probability values of 36.79, 18.39 and 6.13 % respectively.

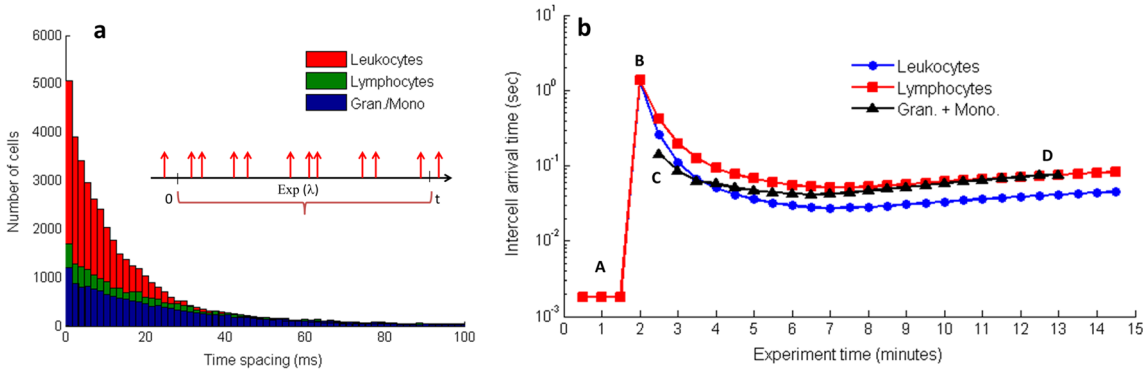

Fig. 6 The time difference in between the cells appearance follows the exponential distribution. **a** The inset shows the spacing in between the cells follow the exponential distribution. The Inter-cell spacing of total leukocytes, lymphocytes and granulocytes+monocytes follows exponential distribution with μ as 47.42, 86.43 and 79.02 msec respectively. **b** The plot shows the μ value of exponential distribution for each minute for the entire experiment duration. (A) Blood Infuses into the chip and lysing and quenching process initiates, no cells appear for initial 2 min, (B) cells gets diffused resulting in higher inter-cell time spacing of 1 sec, (C) granulocytes+monocytes diffused less as compared to lymphocytes and thus appears 30 sec late, (D) granulocytes+monocytes stops appearing 3 min before lymphocytes

3.7 Dilution factor estimation

High concentration of blood cells in the samples requires sample dilution for the accurate counting results. Assuming the initial concentration of the sample is C_0 (cells/μL), with sample flowing at the flow rate of X (μL/min), the time interval, Δt (in seconds) for which λ value is 1, is given as,

$$\Delta t = \frac{60}{C_0\, X} \tag{6}$$

Based on the Poisson theory of counting cells, the required dilution factor (*DF*) can be estimated by the following Equation,

$$DF = \frac{T}{\Delta t\, \lambda_p} \tag{7}$$

where T= *even time seperation coefficient*. Event time is the average time required for the event to occur, e.g. in our case a bipolar pulse width of 80 μs, representing a cell. Separation coefficient is defined as the time spacing (in multiples of event time) required in between two events. λ_p, is the lambda value to get the required Probability P which can be found from the Supplementary Fig. S1. The dilution factor estimation problem can be formulated as to find the dilution factor required using Eqs. 6 and 7 so that no more than 2 cells occur in a time interval with a probability of e.g. 0.5.

4 Discussion

The Poisson counting process characterization can be used for any other particle counting application. Here, we have shown that our cell counting process is a non-homogeneous Poisson

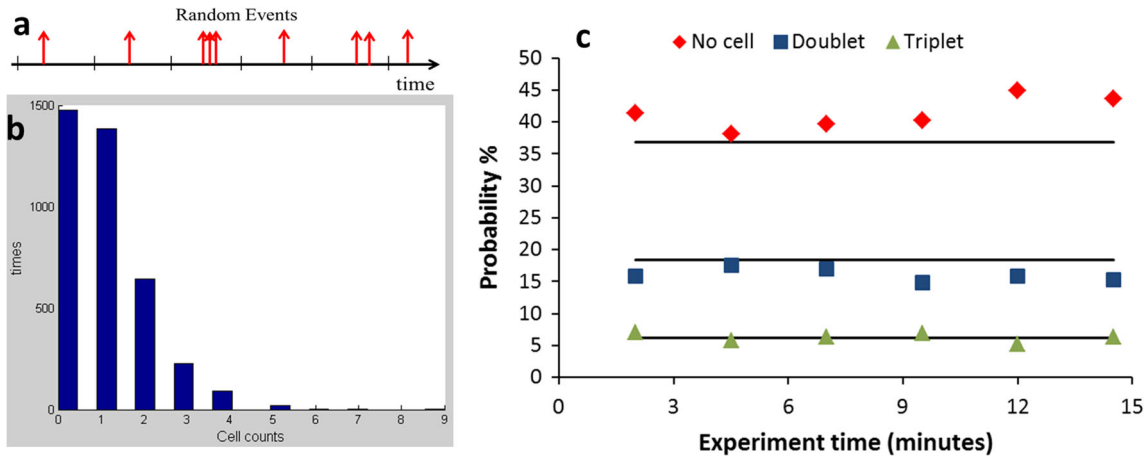

Fig. 7 **a** Occurrence of event clumps follows the Poisson probability function. **b** The Poisson distribution of cell counts for interval of 120 sec. **c** The probability of 0, 2 and 3 cells appearing in intervals of 120 sec for the entire experiment duration of 15 min. The solid black lines represent the theoretical probability values of 36.79, 18.39, and 6.13 % respectively

process, as the λ value changes over time because of the cell diffusion in buffer. However, other particle counting processes can be homogenous Poisson processes provided that there is no diffusion of the particles in the buffer which is pushing the sample in flow based systems. Thus, it is important to characterize the effectiveness of the "push buffer", which can be done by measuring the skewness of the log-normal distribution of the cell/particle counts over experiment time. In samples with heterogeneous cell/particle population w.r.t. size, the diffusion should be characterized for each individual type for accurate counting results. In high particle concentration samples, e.g. erythrocyte counting in diluted blood samples, a portion of the sample is usually selected for cell counting (Berkel 2011). In such applications, characterizing the effectiveness of the buffer by measuring the diffusion of the cells in the buffer is extremely important while selecting the sample portion for accurate counting results.

Coincidence occurrence of cells because of Poisson clumping phenomenon can only be prevented with extremely high dilution factors which makes the counting process impractical. To investigate the multiple occurrences of the cells, the entire experiment time is divided into the time intervals ranging from 2,000 μs to 100 μs and the maximum number of cells were found in those intervals. Fig. S2a shows that the total number of intervals increases exponentially as the time interval bin is reduced from 2,000 μs to 100 μs. The percentage of the intervals with zero cell occurrence increases linearly with (R^2=0.99) as the time interval bin is reduced from 2,000 μs to 100 μs as shown in Fig. S2b. The maximum number of cell occurrences reduces as the time interval bin is reduced as shown in Fig. S3. For the time interval of 100 μs, two cells occur in the bin, verifying a Poisson clumping phenomenon.

5 Conclusions

Particle counting process characterization is important for accurate counting results. In this paper, we characterize the electrical cell counting process in a microfluidic impedance cytometer and is shown to be a non-homogenous Poisson process. We demonstrate that lymphocytes diffused more in buffer as compared to granulocytes and monocytes. In samples with heterogeneous cell populations, individual cell diffusion characteristics should be considered especially if a portion of the sample is being selected for accurate counting results. Our cell diffusion analysis can be used for characterizing buffer effectiveness to push the samples which is critical in accurate cell counting. We also show that the time difference in between the cell occurrences follows an exponential distribution. The probability of occurrence of more than one cell in specified time intervals is also characterized. We used the Poisson statistics to estimate the sample dilution required for samples with high concentrations of cells as this limits the time, throughput, and the volume of the reagents used in the device.

Acknowledgments The authors would like to acknowledge the help of Gregory Damhorst for the blood draw from healthy human donors and Lara Orlandic for help in microfluidic device fabrication.

Funding R. B. acknowledges the support of the NSF NSEC at OSU grant number EEC-0914790, and funding from the University of Illinois, Urbana-Champaign.

References

F. Arqueros, F. Blanco, B.J. Cisneros, Eur. J. Phys. **25**, 399–407 (2004)
C. Berkel, J.D. Gwyer, S. Deane, N. Green, J. Holloway, V. Hollis, H. Morgan, Lab. Chip. **11**, 1249 (2011)
K.C. Cheung, M.Di Berardino, G.S. Kampmann, M. Hebeisen, A. Pierzchalski, J. Bocsi, A. Mittag, A. Tarnok, Cytometry, Part A **77**A, 648–666 (2010)
W.H. Coulter, Means of counting particles suspended in a fluid. US (1953)
R. DeBlois, R.K. Wesley, J. Virol. **23**, 227–233 (1977)
R.W. Glaser, Anal. Biochem. **213**, 152–161 (1993)
U. Hassan, N.N. Watkins, C. Edwards, R. Bashir, Lab. Chip. **14**, 1469–1476 (2014)
D. Holmes, H. Morgan, Anal. Chem. **82**, 1455–1461 (2010)
D. Holmes, D. Pettigrew, C. Reccius, J.D. Gwyer, C. Berkel, J. Holloway, D.E. Davies, H. Morgan, Lab. Chip. **9**, 2881–2889 (2009)
J.J. Kasianiwicz, E. Brandin, D. Branton, D.W. Dreamer, Proc. Natl. Acad. Sci. **93**, 13770–13773 (1996)
R. Kauffman, STLE **45**, 147–153 (1989)
J.F.C. Kingman, *Poisson processes* (Oxford University Press, New York, 1993)
W.L. Leo, *Techniques for nuclear and particle physics experiments* (Springer, Berlin, 1994)
L.W. Phipps, F.H.S. Newbould, J. Dairy Res. **33**, 51–64 (1996)
S.M. Ross, Simulation. (Academic Press, 2006).
O.A. Saleh, L.L. Sohn, Proc. Natl. Acad. Sci. **100**, 820–824 (2003)
T. Sun, H. Morgan, Microfluid. Nanofluid. **8**, 423–443 (2010)
H.A. Teass, J. Byrnes, A. Valentine, Master Brewers Association of the Americas **35**(2), 101–103 (1998).
N.N. Watkins, S. Sridhar, X. Cheng, S.D. Chen, M. Toner, W. Rodriguez, R. Bashir, Lab. Chip. **11**, 1437 (2011)
N.N. Watkins, U. Hassan, G. Damhorst, H. Ni, H., A. Vaid, W. Rodriguez, R. Bashir, Sci. Trans. Med. **5**, 214ra170 (2013).
Z. Zhang, J. Zhe, S. Chandra, J. Hu, Atmos. Environ. **39**, 5446–5453 (2005)